Proton precipitation during magnetic storms in August through November 1998

M. Walt
Starlab, Stanford University, Stanford, California, USA

H. D. Voss
Department of Physics, Taylor University, Upland, Indiana, USA

Received 13 June 2003; revised 15 August 2003; accepted 30 October 2003; published 4 February 2004.

[1] High angular resolution measurements of 155 keV protons were made from the Polar satellite during five magnetic storms in the last half of 1998. Proton precipitation was detected during all the storms studied, and in most cases protons were scattered deep into the loss cone. In one case of strong pitch angle scattering, the fluxes were isotropic for equatorial pitch angles less than 25°. During the main phases of the storms precipitation was strongest at L > 5 on the night side of the Earth, possibly due to field-line curvature scattering of the newly injected ions. During the main and early recovery phases intense precipitation was found in the early afternoon at L > 4 where ring current models predict electromagnetic ion cyclotron waves will be generated by ring current ions. In one storm the nightside precipitation exhibited a maximum near L = 5, and this maximum moved outward during the recovery phase. In most storms the precipitation became less intense as Dst recovered. *INDEX TERMS:* 2716 Magnetospheric Physics: Energetic particles, precipitating; 2778 Magnetospheric Physics: Ring current; 2788 Magnetospheric Physics: Storms and substorms; 2720 Magnetospheric Physics: Energetic particles, trapped; *KEYWORDS:* proton precipitation, magnetic storms

Citation: Walt, M., and H. D. Voss (2004), Proton precipitation during magnetic storms in August through November 1998, *J. Geophys. Res.*, *109*, A02201, doi:10.1029/2003JA010083.

1. Introduction

[2] Major geomagnetic storms are characterized by a depression in the Dst magnetic index due primarily to an enhanced flux of energetic ions and electrons in the trapping region of the magnetosphere. These particles are believed to be injected from the plasma sheet in the geotail by enhanced electric fields which originate in the solar wind [*Chen et al.*, 1993; *Fok et al.*, 1996]. A comprehensive review of ring current formation and decay has recently been published [*Daglis et al.*, 1999].

[3] The recovery of Dst takes place hours or days after minimum Dst, and although changes in various current systems are involved [*Feldstein et al.*, 2000], the major increase in Dst is caused by the removal of ions from the inner magnetosphere. The mechanisms for removal are charge exchange collisions [*Smith et al.*, 1976; *Fok et al.*, 1995], convection through the dayside magnetopause or into the atmosphere [*Liemohn et al.*, 1999; *Kozyra et al.*, 1998], collisional scattering and energy loss [*Jordanova et al.*, 1996; *Fok et al.*, 1991], scattering into the loss cone by electromagnetic ion cyclotron (EMIC) waves [*Cornwall et al.*, 1970; *Jordanova et al.*, 2001; *Khazanov et al.*, 2002], and scattering by field-line curvature [*Sergeev et al.*, 1983; *Anderson et al.*, 1997]. All of these loss processes have been investigated, and the ion removal times have been calculated. However, the wave-particle scattering process is difficult to describe quantitatively, requiring knowledge of the particle anisotropy, of the cold plasma density, of the convective growth rate of the waves as they propagate through the magnetosphere, and of the resonant particle interactions with the wave fields. Estimates of these factors based on simplifying assumptions indicate that wave-particle scattering can be an important loss process immediately inside the plasmapause, particularly in the afternoon Magnetic Local Time (MLT) sector [*Jordanova et al.*, 2001]. However, these estimates do not predict the strong pitch angle scattering postulated by *Cornwall et al.* [1970] and observed by others. [*Hauge and Soraas*, 1975; *Soraas et al.*, 1999; *Walt and Voss*, 2001].

[4] Spacecraft experiments have detected large fluxes of particles, both electrons and ions, precipitating from the ring current into the atmosphere during magnetic storms. [*Williams and Lyons*, 1974; *Lundblad and Soraas*, 1978; *Soraas et al.*, 1999]. These fluxes have been attributed to the scattering of the trapped particles by waves or to changes in the magnetic moment of the ions due to field line curvature [*Sergeev et al.*, 1983; *Anderson et al.*, 1997]. Most of these measurements were made at low altitudes where the loss cone is large so that even moderate angular

0148-0227/04/2003JA010083$09.00

resolution instruments can separate trapped from precipitating particles. However, at low altitude it is not possible to observe a large range of equatorial pitch angles so the overall scattering process cannot be evaluated. Simultaneous measurements of waves and of precipitating protons were made by *Yahnina et al.* [2000] and by *Erlandson and Ukhorskiy* [2001], confirming the association of waves with pitch angle scattering. However, *Erlandson and Ukhorskiy* [2001] did not observe protons above 10 keV, and the angular distributions of the protons did not reach isotropy as required for strong diffusion.

[5] In this paper we report measurements with high angular resolution (±1.5°) of precipitating protons near 155 keV during five intense geomagnetic storms in 1998. Minimum Dst values for these storms occurred on 6 August, 27 August, 25 September, 19 October, and 13 November. The measurements were made from the Polar satellite over a range of latitudes, although the orbit and attitude of the spacecraft favored measurements at latitudes greater than 40°. Some precipitation was seen during all storms although the intensity, L dependence, and the time duration of the precipitation was not the same for all storms.

[6] Section 2 of this paper describes the particle detectors and the Polar satellite trajectory and orbital operations. These factors determine the extent to which this experiment was able to characterize storm-associated precipitation. Examples of precipitating proton data are presented in section 3 along with a description of the precipitation observed in each of the five geomagnetic storms. The comparison of these results with expectations based on current theoretical concepts is given in the discussion section 4. The conclusions derived from these measurements are summarized in the final section 5.

2. Experimental Procedure

[7] The Source/Loss cone Energetic Particle Spectrometer (SEPS) includes two electron and two ion detectors. Only data from the ion detectors will be used here. Each of the SEPS ion detectors consists of a square entrance aperture (3 mm × 3 mm) followed by a focal plane containing 128 silicon solid state detectors arranged in a checkerboard pattern. The separation between the front aperture and the focal plane is 6.59 cm. Each detecting pixel has an active volume 1.3 mm × 1.3 mm × 300 μm thick. Thus, each pixel has an angular resolution of about ±1.5°, and the overall detector has a field of view of about 20° × 20°. The two ion detectors are mounted with their axes antiparallel. When the detectors are aligned parallel to the geomagnetic field, one detector (Zenith) observes downgoing particles and the other detector (Nadir) accepts upgoing ions. Sweeping magnets of about 2 kG are placed across the apertures of the detectors to exclude electrons of energy less than about 2 MeV. These magnets effectively exclude electrons but also deflect incoming 155 keV protons about 2°. An empirical offset was applied to the proton data to compensate for this effect.

[8] Although SEPS is sensitive to all ion species with energies above the detector threshold, it is believed that protons are the dominant ring current ion above 155 keV during magnetic storms [*Kistler et al.*, 1989]. However, *Fu et al.* [2001] reported comparable H^+ and 0^+ fluxes at 150 keV during minimum Dst. In this paper it will be assumed that all ions detected are protons.

[9] Pulses from each pixel were amplified and analyzed by pulse height analyzers covering the energy range 135 keV to approximately 450 keV in eight equal intervals. The data used here are from the lowest energy channel which was centered at 155 keV. Because of the large number of pixels in SEPS it was not possible to provide each pixel with a dedicated pulse height analyzer. Therefore each analyzer serves 16 pixels, sampling each pixel in sequence every 240 μs. This sampling rate determines the individual pixel dead time of 3.8 ms. During the latter half of 1998 the particle detectors accumulated counts for 37 s before reading out the totals. Thus the fluxes reported here are averages over a 37 s time interval.

[10] The silicon sensors were shielded on all sides by a minimum of 1.3 gm cm^{-2} of Ta, Al, and fiberglass. Electronic components and other structures provided additional shielding over about half the solid angle. The minimum shielding excluded protons below about 25 MeV and electrons below about 2 MeV. Since fluxes of 2 MeV electrons occur in the ring current region, penetrating radiation is occasionally a concern as discussed below. The SEPS instrument is described in more detail in the work of *Blake et al.* [1995].

[11] Polar was launched 24 February 1996 into a polar orbit with apogee initially over the North Pole at ~9 Earth radii and perigee at ~1.8 Earth radii. The orbital period was ~17 hours, and Polar passed through the L shells of the trapping region four times in each orbit, two passes in the Northern Hemisphere and two in the Southern Hemisphere. Inbound passes in both the Southern and Northern Hemispheres were at approximately the same MLT, and the outbound passes were about 12 hours different in MLT from the inbound passes. During the summer and fall of 1998 the inbound passes were on the dayside of the Earth and the outbound passes occurred at night. Thus during each orbit Polar made four transits of each accessible L shell, a northern and southern transit at each of two local times.

[12] SEPS is mounted on the despun platform on the Polar satellite. In a typical pass SEPS pointed about 20° off the magnetic field during the Northern Hemisphere inbound pass, pointed nearly parallel to the magnetic field during both inbound and outbound Southern Hemisphere transits, and pointed about 10 degrees off the magnetic field during the northern outbound transit. When the SEPS field-of-view included both trapped and precipitating particles, the structure of the loss cone could be observed and the extent of scattering evaluated. However, at high latitudes (>40°) in the Southern Hemisphere the field-of-view was often entirely inside the loss cone. However, the trapped intensity could be inferred from measurements made at the same MLT and L value on the adjacent Northern Hemisphere transits. An onboard magnetometer, the Magnetic Field Experiment, provided the local magnetic field direction so that SEPS data could be converted to pitch angle distributions.

[13] Shortly after launch SEPS suffered several electronic failures. The amplifiers for the high-energy range failed so that the ion data are limited to the 135 to 450 keV range. The sharing of pulse height analyzers by 16 sensors pixels led to dead time limitations as one pixel with excessive

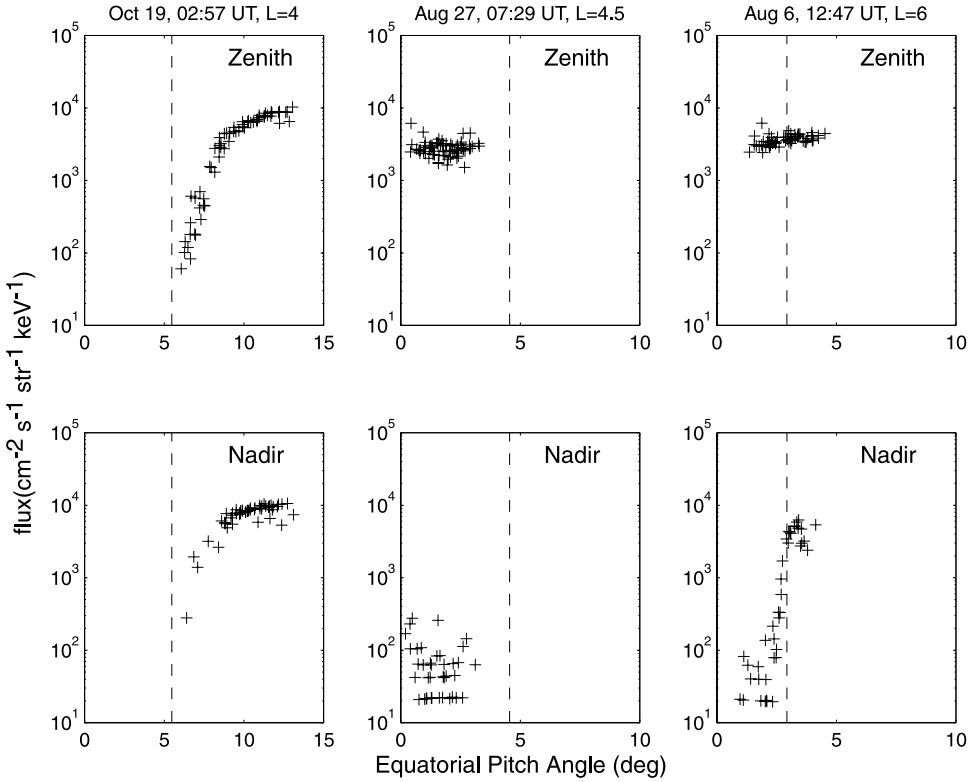

Figure 1. Examples of pitch angle distributions of 155 keV protons measured with SEPS ion detectors at three different dates. Data for the upper panels were obtained by the zenith-pointing detector and indicate downward moving particles. The Nadir detector (bottom panel) faced the opposite direction and records upward moving ions. The vertical, dashed lines denote the atmospheric loss cone angles. Note the strong downward fluxes inside the loss cone in the second and third columns.

noise can reduce the available live time for the other 15 sensors served by the same analyzer. The Si detectors were sensitive to sunlight and earthshine so when either the Sun or the illuminated Earth was in the field of view, the data were degraded. Finally, the electronic noise was much larger than anticipated, requiring a higher detection threshold and limiting the energy resolution. The energy resolution was much larger than the channel width of 39 keV and smoothed any sharp features in the energy spectra. Because of this insensitivity to energy structure the data presented here are all from the lowest energy channel which was centered at 155 keV and had the largest counting rate and the highest statistical accuracy. All the effects listed above have been examined by inflight calibrations. Defective pixels were turned off, and the electronic thresholds were raised well above the noise level. It is believed that the data and interpretations presented in this paper are not affected by the limitations in the SEPS instrument. However, because of uncertainties in the dead time corrections, the magnet deflection corrections and the nonuniformities of individual pixels, the scatter in the data is usually larger than statistical errors.

3. Magnetic Storms of August Through November 1998

[14] During the last half of 1998 five magnetic storms occurred with Dst minima ranging from −112 nT to −155 nT. In addition to a variety of intensities these five storms exhibited different characteristics such as length of recovery phase, presence of a storm sudden commencement (SSC), presence of a two-stage recovery, and presence of multiple minima in Dst. Thus a study of precipitation during these five storms illustrates the variations of the precipitation process under different storm conditions.

[15] Examples of the pitch angle distribution data used in this study are shown in Figure 1, where the three upper panels depict data from the Zenith (upward looking) proton detector and the lower panels give the simultaneous data from the nadir-looking detector. All panels show the differential, directional flux of 155 keV ions (assumed to be protons) as a function of equatorial pitch angle, the transformation from the satellite position to the equatorial plane being accomplished using an offset, tilted, dipole field. The vertical, dashed lines indicate the atmospheric loss cone angles based on a dipole field. In the first example, 19 October 1998 at 0257 Universal Time (UT) both the Zenith and Nadir detectors observe a well defined loss cone, the fluxes inside the loss cone being at least two orders of magnitude below the flux at 12° equatorial pitch angle. This example shows no evidence of precipitation. While convection of ring current protons inward may be transferring some protons into the loss cone, the angular resolution of SEPS is too low to detect such precipitation.

[16] In the other two examples taken on 27 August 1998 and 6 August 1998, the zenith pointing detector observed

fluxes in the loss cone which are one to two orders of magnitude higher than the upward going flux measured by the Nadir detector. These examples show precipitation well inside the bounce loss cone and indicate that the equatorial pitch angle of a proton must change by several degrees in a single bounce. When the satellite is at a high latitude, the transformation to equatorial pitch angles compresses the range of angles measured. Hence at high latitude the range of equatorial pitch angles observed by SEPS is only a few degrees.

3.1. Magnetic Storm of 6 August 1998

[17] On 6 August a magnetic storm with a minimum Dst of −138 nT occurred after almost two weeks of low magnetic activity. The Dst record for this storm is given in the upper panel of Figure 2. Minimum Dst occurred near noon on 6 August, and the slow recovery of Dst over several days was interrupted by a secondary minimum early on 7 August. The three horizontal bars plotted at 17-hour intervals beneath the Dst trace denote time periods when Polar was passing through the inner magnetosphere and sampling the ring current region. Flux records for these time periods are shown in the three panels below the Dst record. During each of these transits SEPS obtained data, generally looking parallel to B while in the Southern Hemisphere. In the Northern Hemisphere the detectors were usually pointed outside the loss cone and measured trapped fluxes. Since the dayside (nightside) Northern Hemisphere passes were at the same MLT as the dayside (nightside) Southern Hemisphere transits, these measurements of trapped and precipitating fluxes were made on nearly the same magnetic field line although at different UT. The magnitude of the flux inside and outside the loss cone gives a measure of the intensity of the scattering process.

[18] Since the SEPS measurements of the 6 August 1998 storm have been described previously [*Walt and Voss*, 2001], the results will be reviewed only briefly here. Plots of the average flux inside the loss cone as a function of L are shown in the lower three panels of Figure 2 for 5, 6, and 7 August 1998. For each day the left-hand panel denotes the Southern Hemisphere inbound pass and the right-hand panel shows the outbound Southern Hemisphere section. Time increases to the right on both left and right panels so the progression through L is reversed. The L values, UT, Magnetic Latitudes, and Magnetic Local Times are shown below each plot. The solid lines denote the fluxes averaged over the loss cone as measured by the Zenith detector, and the dotted line represents average loss cone fluxes seen by the Nadir detector. In cases where the field-of-view did not include the entire loss cone the average flux measured by the pixels inside the loss cone was used. The data end where the detector field-of-view does not include any part of the bounce loss cone.

[19] During the prestorm passes of 5 August 1998, both inbound and outbound passes gave similar L profiles. When the detectors were looking into the loss cones, fluxes from the zenith and nadir were approximately equal and were almost independent of pitch angle. It is believed that the detectors were responding to trapped energetic electrons that penetrated the shielding. The inbound and outbound passes showed similar traces as would be expected for a stably trapped particle population. At this time the High Sensitivity Telescope (HIST) [*Blake et al.*, 1995] also on Polar observed electron fluxes with energies greater than 2 MeV. HIST data have been used throughout this work to identify high background conditions. The identification of precipitation used in this paper is based on the downward fluxes measured by the Zenith detector being much larger than the upgoing fluxes measured by the Nadir detector. On 5 August the differences between upward and downward fluxes are not significant, indicating that during this magnetically quiet time, proton precipitation from the ring current was too small to be detected by SEPS. This subtraction procedure to detect precipitation was sometimes confounded by earthshine, which affected the readings of the Nadir detector. Earthshine can be recognized as it causes highly scattered data points as well as a reduced detector sensitivity.

[20] The precipitating flux during the transits on 6 and 7 August are shown in the bottom two panels. Usually the flux inside the loss cone was almost independent of pitch angle (see Figure 1). On 6 August, precipitation was widespread in L (particularly on the outbound pass at 0430 MLT) and exceeded 10^3 cm^{-2} s^{-1} str^{-1} keV^{-1} from L = 4 to 7.25. The inbound section for 6 August shows a band of precipitation between L = 3.75 and 5.5. The nadir counting rate was much reduced from the prestorm 5 August pass since the high-energy electron background as measured by HIST had decreased during the storm. This reduction of relativistic electron flux during the main phase of storms has been described previously [*Li et al.*, 1999].

[21] On 7 August the precipitation in the afternoon sector increased to greater than 10^4 cm^{-2} s^{-1} str^{-1} keV^{-1} and the precipitation maximum moved inward to L = 4. Again precipitation was not concentrated near any particular L value although there was a sharp inner boundary near L = 4. The L profile of precipitation in the early morning sector (0310 MLT) on 7 August had narrowed in L and was confined to $4.5 < L < 5.25$. On the next Polar pass through the magnetosphere, which took place late on 7 August and early 8 August, no precipitation was detected at any L value.

[22] The strong precipitation (flux > 10^4 cm^{-2} s^{-1} str^{-1} keV^{-1}) in the afternoon MLT sector on 7 August 1998 is noteworthy in that the precipitating fluxes are comparable to the trapped fluxes. On the inbound section of the orbit SEPS measured trapped particles in the Northern Hemisphere and about 1 hour later observed precipitating fluxes at the same L shells in the Southern Hemisphere. Since the inbound portion of the pass takes place at almost constant MLT these Northern and Southern Hemisphere measurements are on nearly the same field lines.

[23] Pitch angle distributions obtained during the Northern and Southern Hemisphere sections of the inbound pass on 7 August are presented in Figure 3 for L = 4.0, 4.5, 5.0, and 5.5. Data for equatorial pitch angles greater than 8° represent trapped particles and were measured in the Northern Hemisphere section of this pass. Fluxes at less than 5° pitch angle are precipitating protons and were obtained in the Southern Hemisphere about one hour later. Above L of about 4.5 the trapped and precipitating fluxes are nearly equal, indicating that scattering has filled the downward loss cone.

[24] On the outbound section of this orbit, which passed through the Southern and Northern Hemispheres at about 0330 MLT, the precipitating fluxes measured in the south

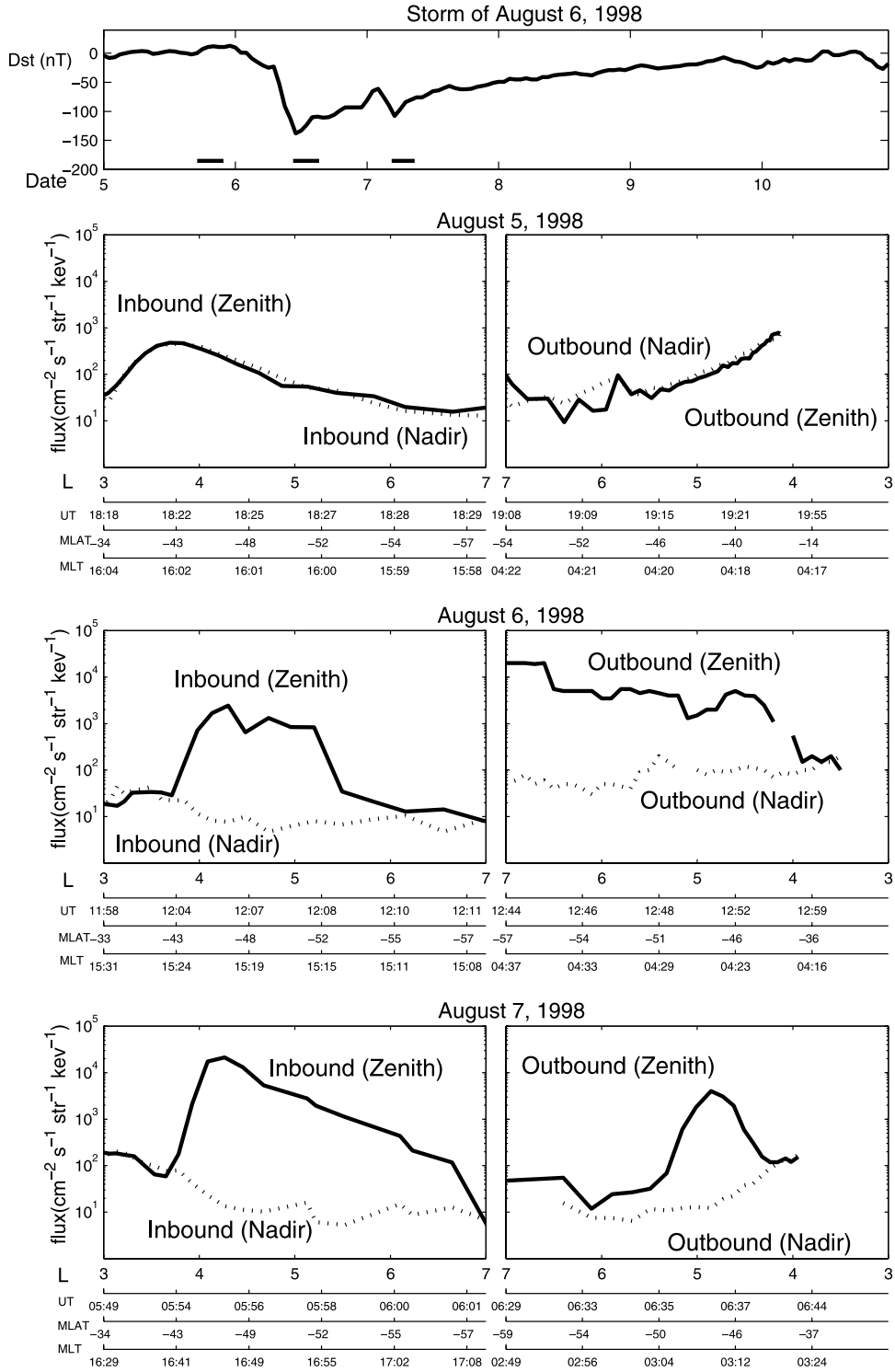

Figure 2. Magnetic storm of 6 August 1998. Top panel shows Dst index. The bars near the horizontal axis denote times when POLAR was inside the trapping region and able to observe ring current ions. The lower panels give the precipitating fluxes observed in the Southern Hemisphere during the inbound passes (left hand column) and outbound passes (right hand column). Solid lines are average loss cone fluxes as observed by the Zenith detector and the dotted lines represent loss cone fluxes seen by the Nadir detector. Note that UT increases towards the right in both columns.

were a factor of ten less than the trapped fluxes observed in the north.

[25] The isotropic fluxes are believed to be part of the ring current population and not fluxes of solar energetic protons that are produced at the sun and enter the magnetosphere during magnetic storms. Contrary to expectations for solar energetic protons, the fluxes observed here decrease with increasing L and at

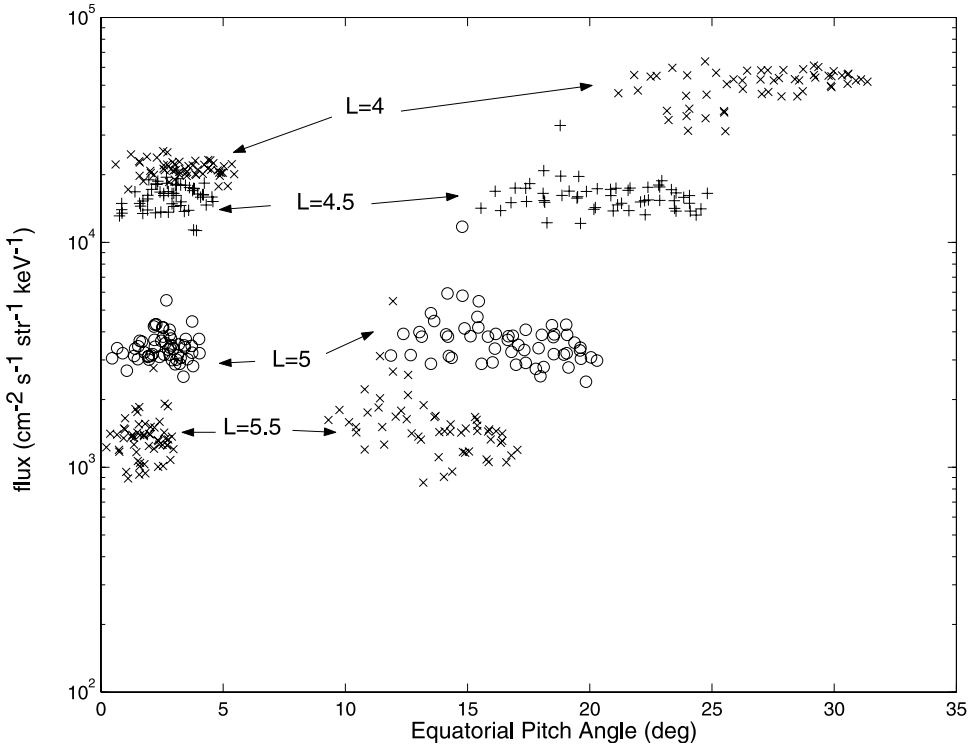

Figure 3. Equatorial pitch angle distributions of downward moving protons on the inbound pass of 7 August 1998. Fluxes at angles below 5° were measured in the Southern Hemisphere while the trapped fluxes at pitch angles greater than 10° were measured about 1 hour earlier in the Northern Hemisphere.

L = 10 are insignificant in both Northern and Southern Hemispheres.

3.2. Magnetic Storm of 27 August 1998

[26] The magnetic storm late in August 1998 began with an SSC on 26 August followed by a slow decrease in Dst reaching minimum Dst of −155 nT near 1000 UT on 27 August. Figure 4 presents Dst and the precipitation data for this storm in the same format as Figure 2. No precipitation was seen midday on 26 August, but in the first pass on 27 August, near Dst minimum, substantial precipitating fluxes were seen in both the afternoon and early morning MLT sectors. The pattern of precipitation on 27 August is quite similar to that of 6 August in that the L profile for the morning sector shows strong precipitation extending to L = 7. In the afternoon MLT sector the precipitation is most intense in the central ring current region, near L = 4.5, and does not extend outward beyond L = 5.5, similar to the afternoon precipitation on 6 August.

[27] The next pass of Polar through the ring current region occurred early on 28 August after Dst had recovered to −60 nT. The precipitating fluxes in the night sector (0130 MLT) had decreased at high L but continued to be intense near L = 5. On the inbound pass in the afternoon sector substantial precipitating fluxes were observed only above L = 5. The high counting rates near L = 3 were seen in both the Zenith and Nadir detectors and are due to penetrating particles. The precipitation further decayed by late in the day of 28 August (Figure 4, bottom panel) when another transit recorded precipitation only at L > 6 in both morning and afternoon MLT sectors. On 29 August the precipitation was too small to measure.

3.3. Magnetic Storm of 25 September 1998

[28] The magnetic storm of 25 September 1998 began with a sudden commencement shortly after midnight and a rapid decrease in Dst to −207 nT at 1000 UT (top panel of Figure 5). This Dst value is the lowest value of the five storms studied here. The phasing of the Polar orbit was fortunate in that Polar passed through the inner magnetosphere during the minimum of Dst. The inbound Southern Hemisphere transit on 25 September occurred at about 1248 MLT and the outbound Southern Hemisphere pass was near midnight (0122 MLT). During the inbound Southern Hemisphere pass, the precipitation was widespread, extending from L = 4.2 to beyond L = 6. Below L = 4 on the inbound section the Sun was in the field of view of the Zenith detector, and the detector response was reduced. The dashed line in the second panel of Figure 5 shows the reduced detector response at the time of sunlight illumination. During the inbound pass the Nadir detector fluxes are anomalously low and scattered, probably due to earthshine. On the outbound (nightside) section precipitation was encountered above L = 5.25. No precipitation data were available below that L value as SEPS was not oriented to view the loss cone.

[29] The next pass of Polar through the inner magnetosphere took place early on 26 September, when Dst had recovered to −50 nT. In the inbound Southern Hemisphere pass, which occurred near 1412 MLT, the precipitation pattern

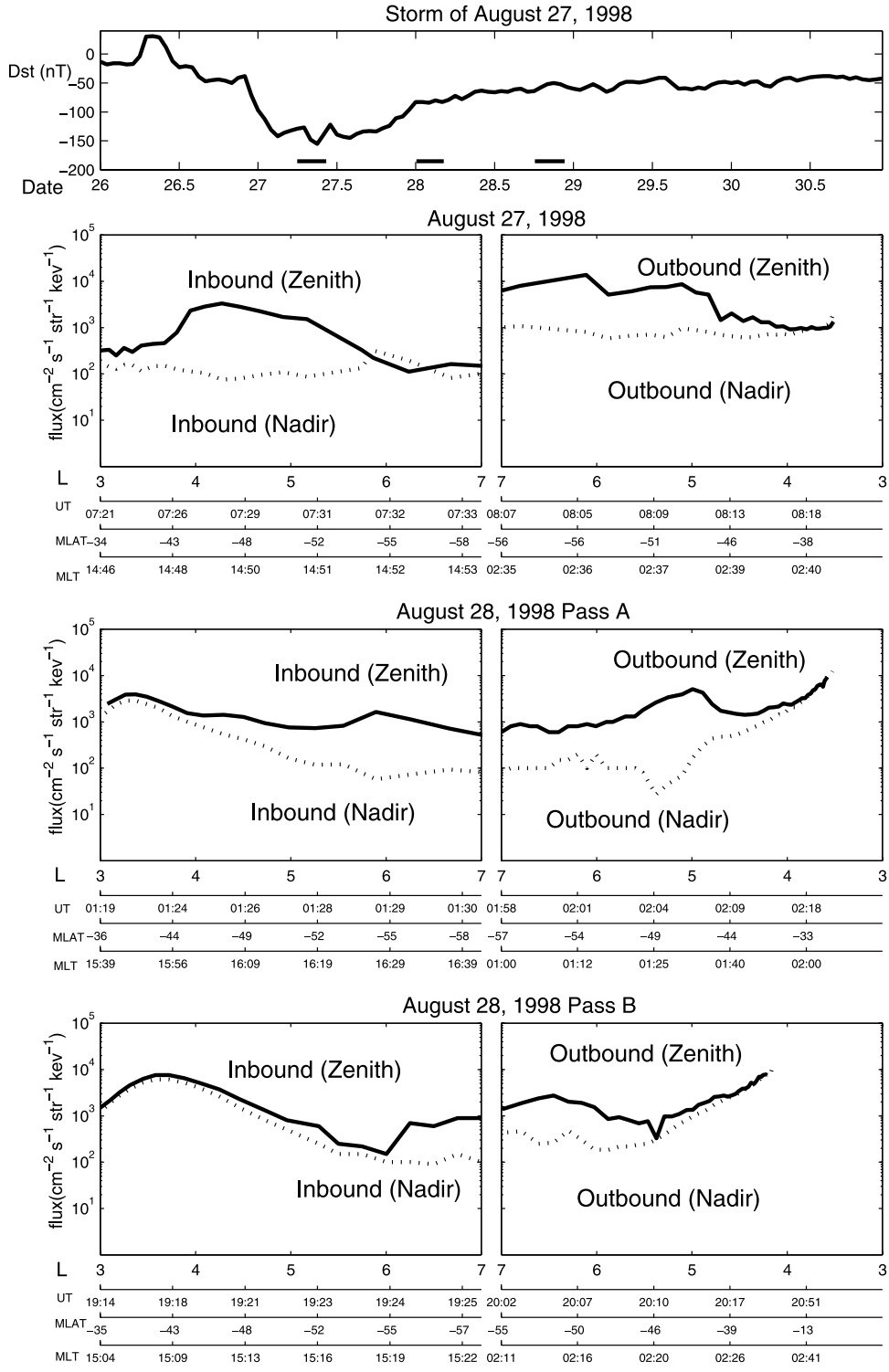

Figure 4. Magnetic storm of 27 August 1998. Same format as used in Figure 2.

had decayed to prestorm values. The nadir counting rates (not shown) were negligible due to earthshine in the Nadir detector. The zenith fluxes correspond to quiet time penetrating particle counts. On the Southern Hemisphere outbound pass at 2330 MLT precipitation was moderate at L = 5 but was greatly reduced beyond L = 5.5. Unfortunately, on this transit SEPS was not oriented to view the loss cone below L = 4.9.

[30] The next transit of the magnetosphere was late in the day on 26 September 1998. On the inbound pass through the Southern Hemisphere the upward and downward fluxes were approximately equal and the overall pattern followed the intensity of the penetrating background. On the outbound pass no precipitation data were obtained below L = 6.25 as the despun platform orientation did not allow SEPS

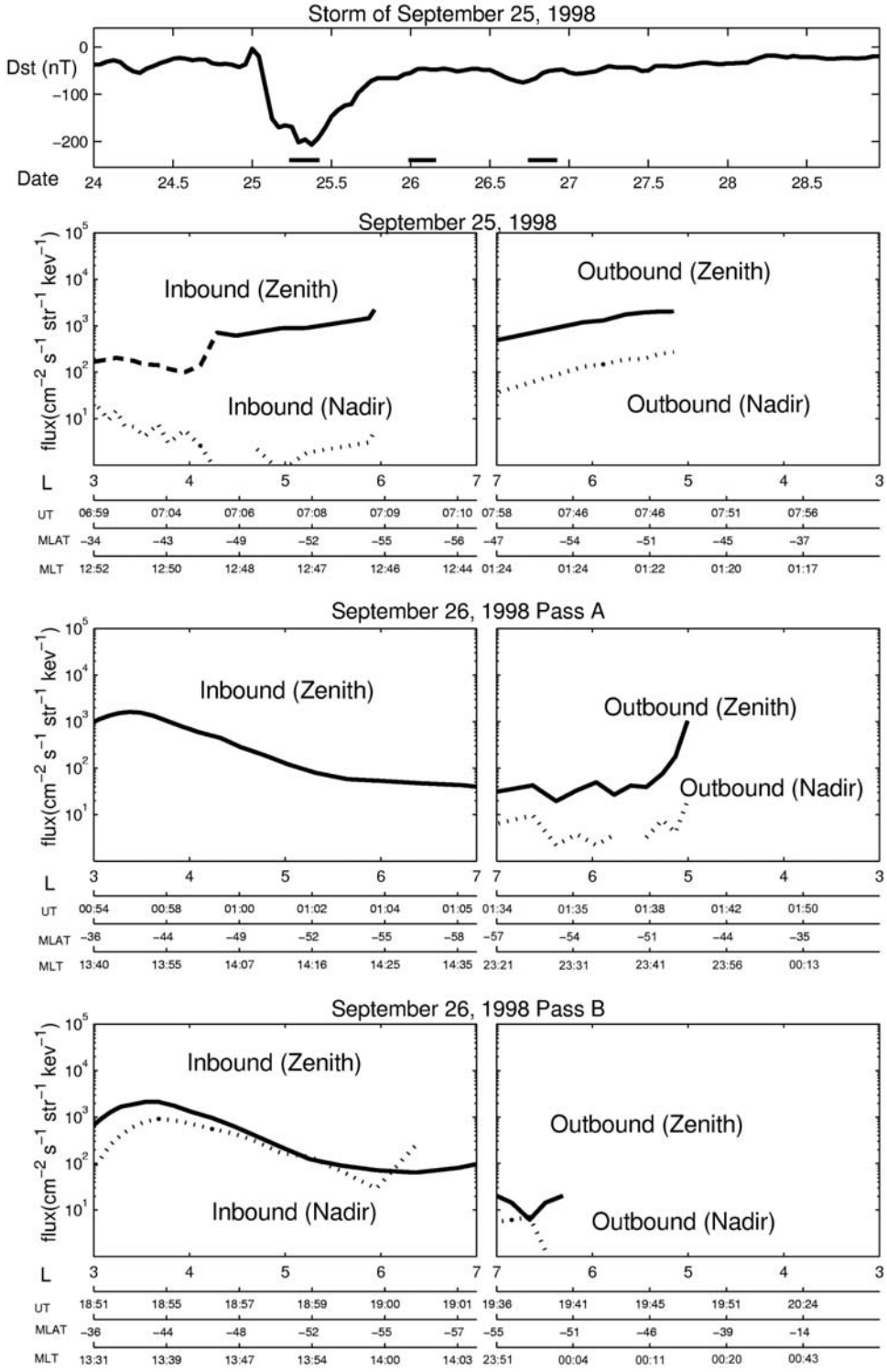

Figure 5. Magnetic storm of 25 September 1998. Same format as used in Figure 2.

to view inside the loss cone. Thus no precipitation was detected on the second pass of 26 September 1998.

[31] The initial precipitation during the 25 September storm was widespread and at high L values, similar to that of the storms in August. Above L = 4.25 on the dayside the flux intensity was a maximum of a few times 10^3, a factor of 10 less than the trapped flux measured in the conjugate hemisphere. Therefore even though Dst was large during this storm strong diffusion was not present, at least during times when Polar was passing through the ring current region. The lack of substantial precipitation on 26 September is not surprising as Dst had largely recovered by that time.

[32] The 25 September storm has been simulated by *Daglis et al.* [2003]. Although their model did not include precipitation by EMIC waves, their calculated Dst values

closely matched experiment, implying that wave-particle losses were not important in this storm.

3.4. Magnetic Storm of 19 October 1998

[33] The storm that took place on 19 October 1998, began with a rapid decrease in Dst to −112 nT. The initial recovery to −30 nT occurred within one day although Dst fluctuated for another week before it was consistently above −10 nT. At this time the Polar orbit was very nearly in the noon/midnight meridian plane with its spin axis perpendicular to the orbital plane. Since SEPS pointed perpendicular to the Polar spin axis, its field-of-view was in the noon/midnight meridian. For some settings of the platform angle it was therefore possible for either the Zenith or Nadir detector to view the sun directly, usually in the midlatitude portions of the Polar orbit.

[34] Polar made two transits of the southern magnetosphere on 19 October, one between 0200 and 0300 UT and one late in the day between 2000 and 2100 UT. In the first pass SEPS was pointed away from the field line on the Northern Hemisphere segment and no precipitation information was obtained. On the inbound Southern Hemisphere segment (Figure 6, panel 2) precipitating fluxes below 100 cm^{-2} s^{-1} str^{-1} keV^{-1} were seen near L = 6 although these low values are near the limit of detectability. On this pass data below L = 5.0 were lost as the sun was in the SEPS field of view. However, in the Southern Hemisphere outbound pass near MLT = 2250 precipitating fluxes of 1–2 × 10^3 cm^{-2} s^{-1} str^{-2} keV^{-1} were measured. Thus early in the storm precipitation was concentrated in the nighttime sector, predominantly at L > 4.5. The trapped flux measured 2 hours later on the same field lines in the Northern Hemisphere outbound section was only 500 cm^{-2} s^{-1} str^{-1} keV^{-1}, suggesting that the trapped flux probably decreased in the 2-hour interval between Southern and Northern transits.

[35] The next orbit of Polar through the radiation belts took place near the end of the day on 19 October (Figure 6, third panel). In contrast to the first pass 18 hours earlier, most of the precipitation was observed on the inbound segment on the noon side. Precipitating fluxes of 300 to 500 cm^{-2} s^{-1} str^{-1} keV^{-1} were measured between L = 5.5 and 7.5. On the outbound segment after 2056 UT the despun platform was not oriented to see precipitation below L = 4.8, and at higher L the zenith and nadir fluxes were approximately equal.

[36] The next day, 20 October, Polar passed through the southern radiation belt region between 1400 and 1515 UT. On the inbound pass no data were obtained in the Northern Hemisphere due to sunlight illuminating the Zenith detector. In the Southern Hemisphere section of the inbound pass weak precipitation between 50 and 200 cm^{-2} s^{-1} str^{-1} keV^{-1} was seen between L = 3.8 and 4.5. No downgoing protons were detected above L ≈ 5.0. On the outbound portion of the Southern Hemisphere orbit, which occurred at 2323 MLT, precipitation was only found near L = 6. Below L = 5.56 the position of the despun platform did not allow measurements at equatorial pitch angles below 5°. In the Northern Hemisphere section of the outbound pass the despun platform attitude was changing rapidly and SEPS acquired no useful data. Therefore on 20 October the only precipitation observed was very weak and confined between L = 3.5 and 5 at 1126 MLT and near L = 6 at 2323 MLT. It is possible that precipitation was present below L = 5.5 on the outbound Southern Hemisphere pass but was not seen because of the platform angle.

[37] The 19 October 1998 storm had the smallest |Dst| of the five storms reviewed here. The precipitation was also the least impressive of the storms, having a maximum precipitating flux of 2000 cm^{-2} s^{-1} str^{-1} keV^{-1} near midnight MLT on 19 October at L = 6.75, well beyond the normal ring current region. This precipitation occurred slightly before minimum Dst and was short lived since the precipitation measured on the next outbound pass of 19 October, was too small to be reliably detected.

[38] The orbital phasing of Polar was unfortunate for this storm in that no transit of the radiation belts occurred at minimum Dst. Also, the alignment of the orbital plane with the noon/midnight meridian frequently allowed the Sun to disable the detectors.

3.5. Magnetic Storm of 13 November 1998

[39] This storm exhibited a slow decrease in Dst taking almost a day to reach the minimum value of −131 nT. The recovery of Dst was also slow and extended over the next three days. (Figure 7, top panel)

[40] On November 13 Polar transited the radiation belt region before the minimum in Dst occurred, and no appreciable precipitation was observed on the inbound orbit, the counts in the Zenith detector being attributed to penetrating electrons (Figure 7, second panel). The Nadir detector was strongly affected by earthshine on all inbound passes for this storm, and the measurements are therefore not shown. On the outbound (night) section of the orbit, as Polar was moving from the South Pole towards the equator and L was decreasing, both the trapped and precipitated flux increased abruptly at L = 4.3. This sudden increase is probably a time variation in flux rather than a structure in L and indicates the arrival of injected flux at the satellite location. Below L = 4.1 SEPS turned away from the field line and was unable to see the loss cone. On 14 November, two passes through the belts occurred, the first between 0315 and 0415 UT and the second between 2115 and 2215 UT. (Figure 7, third and forth panels). The earliest pass (Pass A) encountered precipitation on both the inbound (0934 MLT) and outbound segments (2200 MLT) in the Southern Hemisphere. Inbound, the precipitation was above L = 5.5. Outbound, precipitation extended above L = 4. The nadir loss-cone fluxes at this time were too small to measure. The second pass (Pass B) found precipitation only on the nightside, outbound sector. The nighttime precipitation on pass A had a pronounced maximum at L = 4.25 which may be related to the sharp increase seen at L = 4.25 on the previous day. In the second pass on 14 November the precipitation was large at 2018 MLT and was concentrated between L = 4.5 and 6.5.

[41] The pass through the southern radiation belt region on 15 November (Figure 7 bottom panel) occurred between 1515 and 1715 UT, 2 days after minimum Dst. In the daytime sector (1050 MLT) the L profile resembled the penetrating background seen at other times, so it is probable

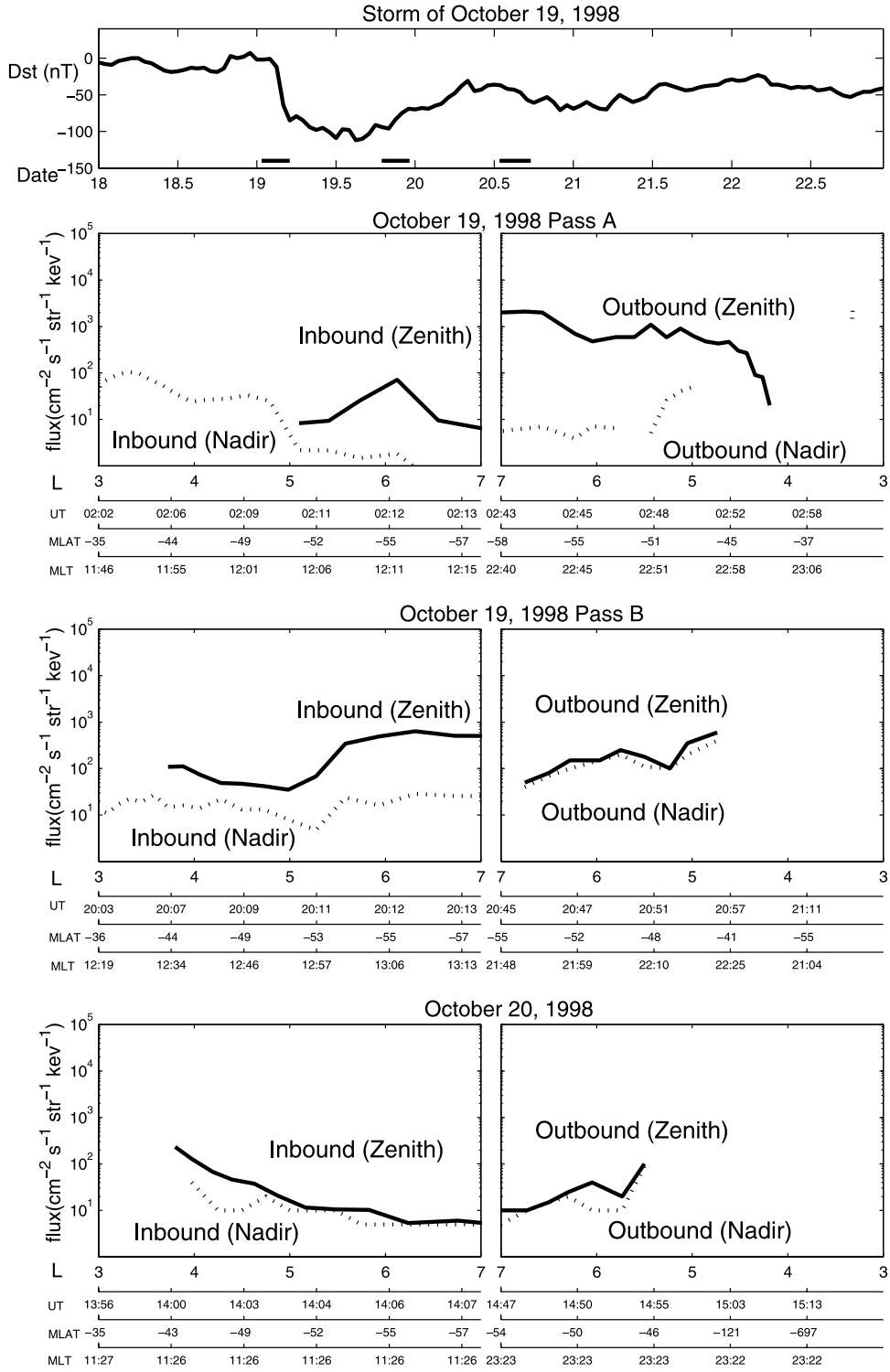

Figure 6. Magnetic storm of 19 October 1998. Same format as used in Figure 2.

that little, if any, precipitation occurred on this pass. In the nighttime sector on the outbound portion of the orbit a pronounced maximum in the precipitation was seen at L = 5.1. If the peaks seen on 13, 14, and 15 November are related, they exhibit a continuous movement of the precipitation outward in L.

[42] On the next day, 16 November (not shown), the nightime precipitation was still present in the region near L = 5.1, but the peak fluxes had decreased by a factor of 3. The 13 November magnetic storm was notable in that proton precipitation continued for 3 days after the Dst minimum. The precipitation pattern was also unusual in that during recovery the night side precipitation exhibited a maximum which moved from L = 4.2 to 5.1. This maximum persisted throughout the storm and on Nov 15 had a full width at half maximum of $\Delta L = 0.5$. This narrow precip-

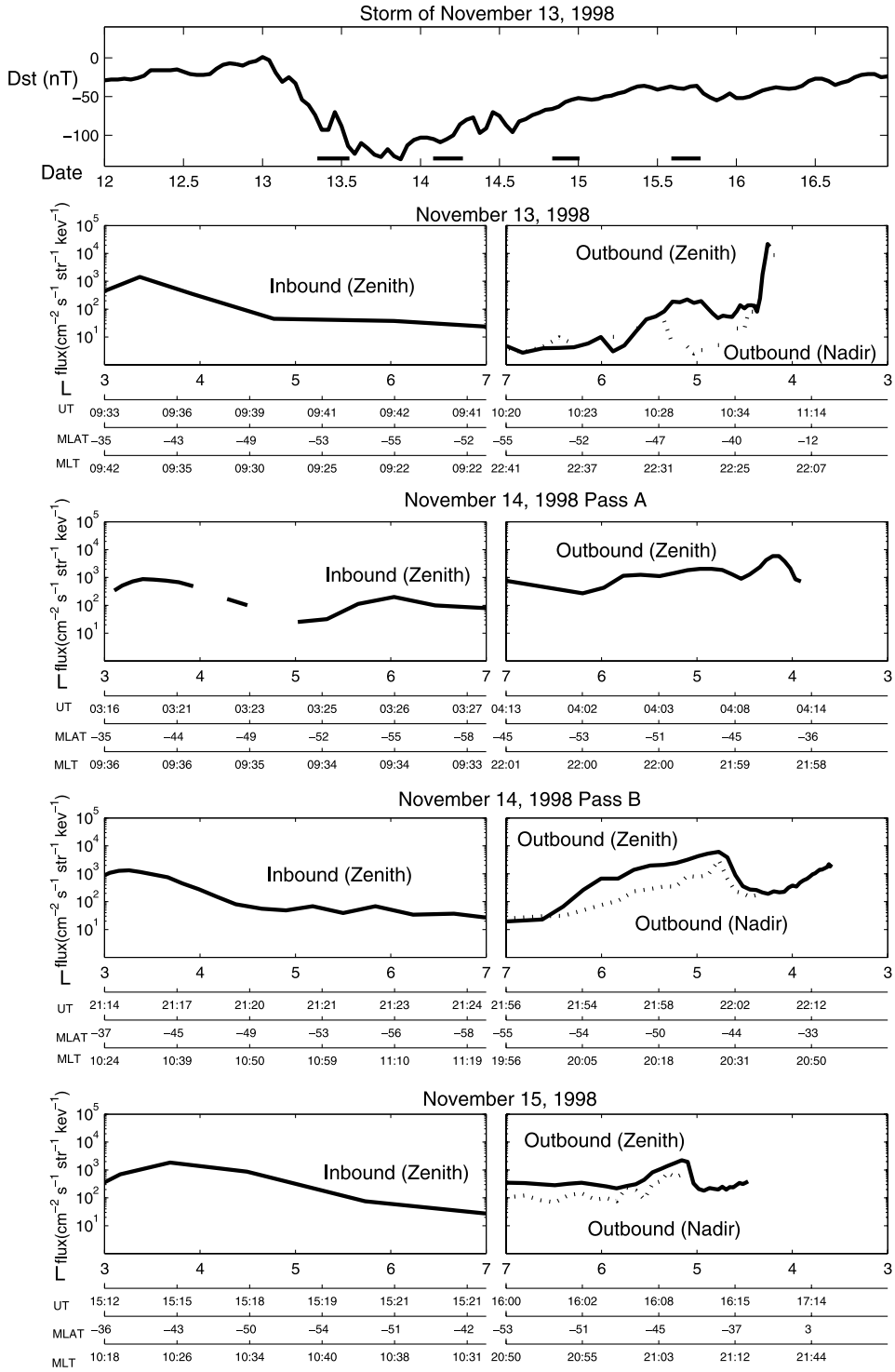

Figure 7. Magnetic storm of 13 November 1998. Same format as used in Figure 2.

itation region is similar to the structure reported by *Soraas et al.* [1999] from measurements with a low-altitude polar orbiting satellite.

4. Discussion

[43] In the measurements reported here precipitation of ring current protons was commonly found during the main and recovery phases of magnetic storms. Before drawing conclusions from these measurements it is useful to review the constraints of the SEPS instrument and the POLAR orbit. The lowest-energy channel available had its midpoint energy at 155 keV so only the high-energy portion of the ring current was observed. Also, the time and spatial sampling of each storm was limited by the Polar orbit, by the orientation of the instrument platform, and in some cases

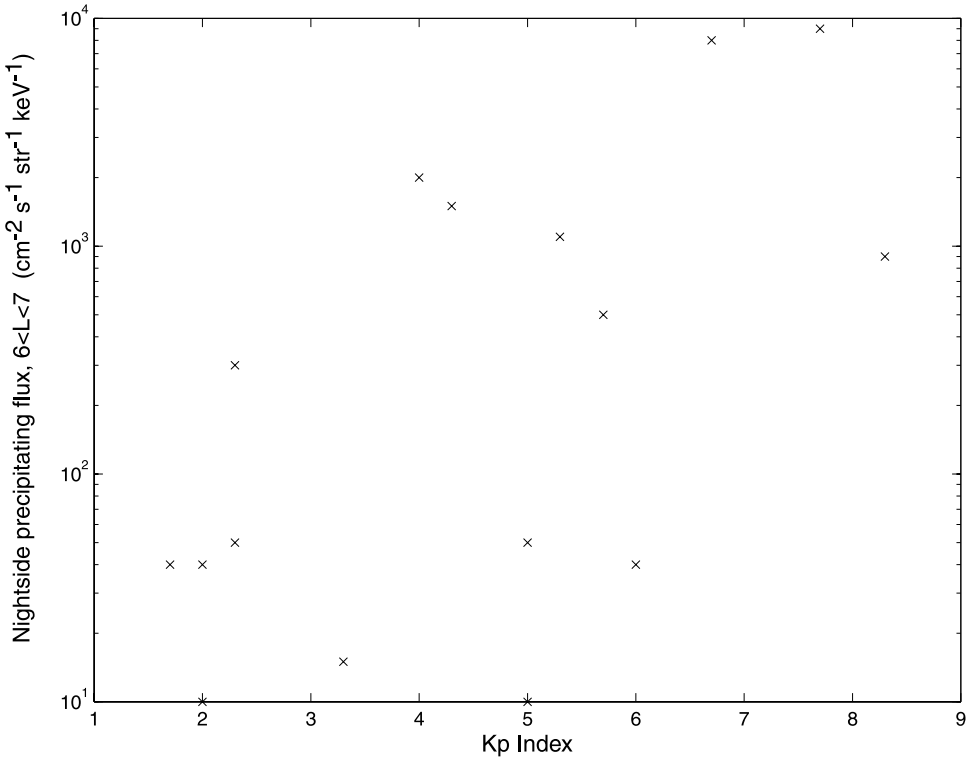

Figure 8. Scatter plot of average nightside precipitation between L = 6 and 7 as a function of Kp for the 3 hour interval inclosing the satellite passage. Kp is a proxy for particle injection into the ring current and the increase in precipitation with Kp indicates that the precipitation accompanies injection.

by sunshine or earthshine interference. Polar crossed the ring current region at two MLT values during each 17-hour orbit. Thus for a single storm it was not possible to measure the dependence of the precipitation on MLT. However, since the storms studied occurred over a 4 month interval, the precession of the Polar orbit allowed SEPS to sample several local times, although for different storms. In the five storms studied precipitation was observed at local times on the dayside between 0940 MLT and 1650 MLT and on the nightside between 2006 MLT and 0304 MLT. Thus the sampling was not uniform, and in particular precipitation data are not available near the dawn and dusk sectors.

[44] In all the storms studied, substantial precipitation occurred for L > 4. Since these measurements were usually made away from the equator and the downward flux greatly exceeded the upward moving protons, the scattering region must have been located toward the equator from the satellite. The strong contrast between upward and downward going fluxes and the generally flat angular distributions inside the loss cones indicate that the protons must have been scattered by several degrees during a single bounce period. This magnitude of pitch angle change is not possible by coulomb collisions alone [*Jordanova et al.*, 1996] or from convective drift. In some cases (for example 7 August at L = 4.5, Figure 3) the angular distribution of the proton flux was nearly isotropic for equatorial pitch angles below 25° as would be the case for strong diffusion [*Kennel and Petschek*, 1966]. Under strong diffusion the trapping lifetime of 155 keV protons would be about 15 min. The overall time scale for the decay of the ring current would, of course, be longer since scattering of this intensity occurred over a limited L range and probably did not take place at all local times. Furthermore, injection of new particles could be replacing the precipitation losses.

[45] There are some similarities in the morphology of precipitation during the different storms, although Polar encountered the different storms at different MLT and during various phases of the storm development. During the main phases the precipitation during the nightime sections of the orbit was usually larger than on the dayside and extended to larger L values. This behavior is illustrated by the data for 6 August, 27 August, 19 October, and to a lesser extent on 25 September. (On 13 November, Polar passed through the high L shell before Dst minimum, and it is possible that the injection and precipitation had not fully developed.) This main phase night side precipitation occurs at the time particles were injected into the ring current.

[46] A comparison of night side precipitation with Kp, a proxy for particle injection provides some confirmation of the expected relationship between injection and precipitation. In Figure 8 the average precipitation between L = 6 and 7 on the night side during the main phases of the five storms is plotted against Kp for the 3 hour intervals enclosing the satellite passes. In spite of the large scatter there is an increase in nighttime precipitation with increasing Kp. (The lowest point at Kp = 5, flux = 10 represents the 13 November transit and is misleading since the outbound pass through 6 < L < 7 occurred before the precipitation had developed.)

[47] In the recovery phase nightside precipitation at L ≈ 6 decreased while dayside precipitation at L ≈ 4 usually increased. In the recovery phases of the storms, the

precipitation region on the nightside occasionally became restricted in L as illustrated in Figure 2 for 7 August, Figure 4 for 28 August, and Figure 7 for 14 and 15 November. The November storm is particularly interesting in that the maximum in nightside precipitation appears to move outward in L during recovery. The September storm does not show this behavior as the recovery was rapid and was almost complete before the first Polar transit on 26 September.

[48] The time duration of the precipitation was different for the various storms but generally corresponded to the recovery time of Dst. For example precipitation was intense on only one Polar orbit for the 25 September 1998 storm, which had a rapid recovery. The slow recovery of Dst during the 13 November 1998 storm was accompanied by appreciable precipitation for four orbits over 3 days. Evidently, a large ring current and therefore a low Dst is required for precipitation to occur.

[49] While these data consist of intermittent measurements of only five storms, they may be compared with the precipitation predicted by magnetic storm models. Extensive simulations of the precipitation during magnetic storms have been done by *Kozyra et al.* [1998], *Liemohn et al.* [2001], *Daglis et al.* [2003], *Jordanova et al.* [2001], and *Khazanov et al.* [2002]. The last two references are particularly pertinent as the authors explicitly treated precipitation of protons by EMIC waves. These authors computed the pitch angle distributions of drifting ions, constructed a plasmasphere model, calculated the wave growth rate in the anisotropic particle distributions, allowed the ions to diffuse in the wave field, and thus obtained the precipitating flux as a function of proton energy, L, MLT, and time during the storm. The simulations generally show proton precipitation in the night side region and in the midafternoon MLT sector. The nightside precipitation is attributed to inward convective drift of the newly injected protons, and this precipitation occurs even in the absence of waves. The nightside precipitation observed with SEPS is probably not caused by convective drift as the particles are found deep inside the loss cone, indicating that the equatorial pitch angles were changed several degrees in one bounce. A plausible explanation for the SEPS results is that the newly injected protons were scattered by field line curvature effects as they passed through the distorted magnetic field near the equatorial plane. *Anderson et al.* [1997] have calculated the onset of field line curvature scattering in a distorted field and find that for Kp = 6 appreciable scattering of 155 keV protons can occur at radial distances of 5 Earth radii in the tail. With this mechanism precipitation is indicative of a ring current source rather than a ring current loss [*Soraas et al.*, 2002]. The magnetic storm simulations referred to above did not include scattering by field line curvature.

[50] The change in precipitation with L on the night side can be very abrupt as exemplified by measurements on the outbound pass on 15 November near L = 5. Pitch angle distributions from adjacent frames taken 37 s apart are plotted in Figure 9. The left panel for L = 5.07 shows a clear loss cone for 155 keV protons. In the right hand panel, for L = 5.11 and observed 37 s earlier, the proton distribution fills the loss cone. Although it is not possible to identify this change as temporal or spatial, its occurrence late in the storm suggests it is a spatial effect. In this case the precipitation is caused by a change in the pitch angle distribution rather than an overall increase in flux since the flux at 6° (outside the loss cone) is unchanged.

[51] In the simulations intense precipitation in the early afternoon sector was produced by waves, which were driven by the anisotropic trapped proton distributions. This prediction agrees with our observations of intense precipitation at 1520 MLT on 6 August and at 1630 MLT on 7 August. However, in the simulations the scattering was not strong enough to drive the distribution to isotropy as was observed. The simulations predict only light precipitation before noon on the dayside. In contrast the SEPS pass on 14 November at about 0930 MLT showed appreciable precipitation at L > 5.5.

[52] In some ring current models precipitation is predicted to be strongest near the plasmapause where the EMIC waves were guided by the cold plasma density gradients. The precipitation followed the plasmapause, moving inward during the main phase and moving outward during the recovery phase as the plasmasphere refilled. The outward motion of precipitation during 14 and 15 November may correspond to this prediction although it is not known where the plasmaspause was during this time. Using the prescription of *Carpenter and Anderson* [1992], which relates the plasmapause location to the maximum Kp value during the preceding 24 hours, the plasmaspause should be 1 to 2 Earth radii inside the precipitation location. However, this prescription is of questionable value during highly disturbed conditions, and detached plasma regions, which could promote precipitation, are often found outside the predicted plasmapause location (D. Carpenter and M. Spasojevic, private communication, 2003).

[53] The ring current models predict the strongest dayside precipitation near Dst minimum when the ring current is well populated. We find that the most intense precipitation did not always occur at minimum Dst although the samples were taken at only two MLT values during each storm, and these times were different for each storm. In the 6 August storm, the maximum precipitation was observed on 7 August, almost a day after minimum Dst. (However, there was a secondary dip in Dst near the time of greatest precipitation). In the 13 November storm the nightside precipitation peak near L = 5 reached its largest value late on 14 November. On the other hand the 27 August storm showed maximum precipitation during the broad Dst minimum.

5. Summary and Conclusions

[54] During the main and recovery phases of intense magnetic storms (Dst < 100 nT) large fluxes of >155 keV protons were often found inside the bounce loss cone. In one case the pitch angle distributions were nearly isotropic for equatorial pitch angles less than 25° indicating that strong pitch angle scattering was taking place. Under strong scattering the local trapping lifetime is about 15 min. In most cases the pitch angle distributions appeared isotropic inside the loss cone although the trapped flux at larger pitch angles was greater. The scattering of protons by several degrees during half a bounce period is larger than can be accounted for by convective drift or by Coulomb collisions.

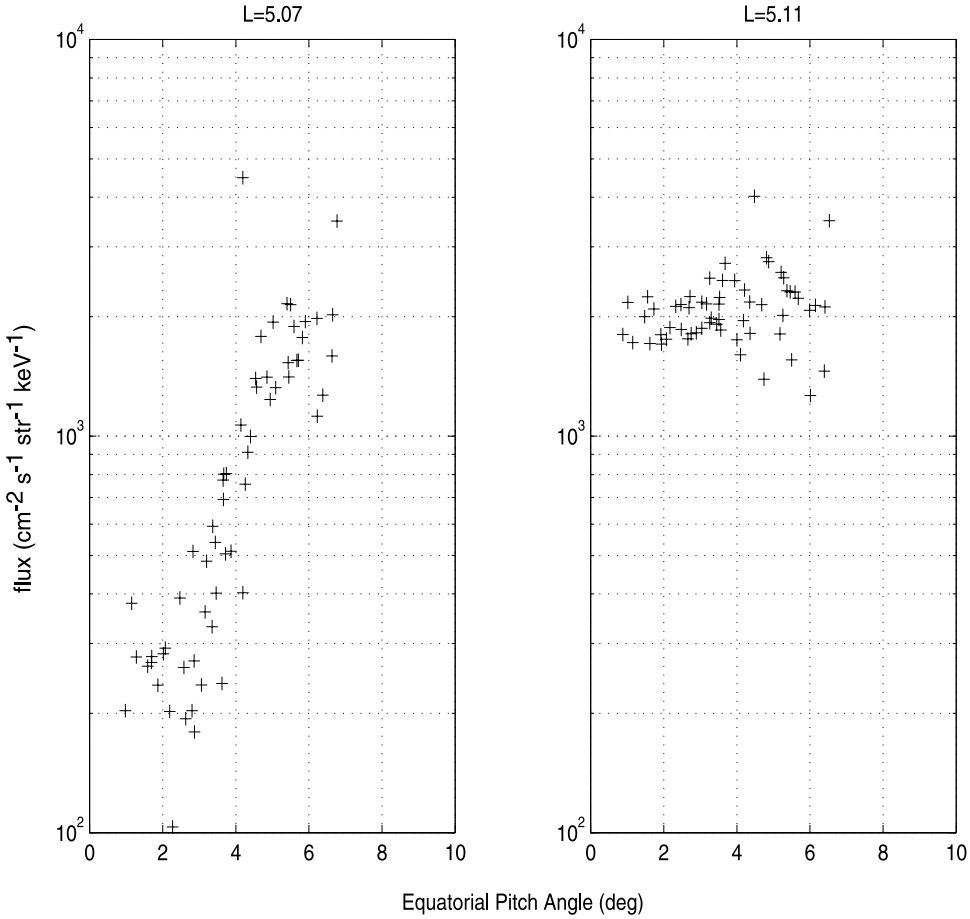

Figure 9. Pitch angle distributions observed 37 s apart on the outbound pass on 15 November. Note the well-defined loss cone for 155 keV protons at L = 5.07 and the filled loss cone at L = 5.11.

[55] The precipitation is frequently widespread, extending over several units of L. The widespread nature of the precipitation was most noticeable near midnight during the main phase of the storm. This initial precipitation may result from injection on distorted field lines where protons can be scattered into the loss cone by field line curvature effects.

[56] On the dayside the most intense precipitation was found in the afternoon sector at $4 < L < 6$ during the main and early recovery phase. This region of precipitation is where ring current models predict precipitation by EMIC waves. However, most models limit the growth of waves and thus preclude the occurrence of strong diffusion. The time duration of precipitation generally followed the trend of Dst. When Dst recovered rapidly, the precipitation was also short lived.

[57] In one storm of long duration (13 November 1998) a maximum in the L distribution of precipitation was found on the night side during the recovery phase. This maximum moved outward during the recovery phase as predicted by simulations where EMIC waves are guided by the plasmapause.

[58] **Acknowledgments.** The authors gratefully acknowledge the contributions of J. Mobilia of the Lockheed Martin Corporation for in-flight commanding of the SEPS instrument on the Polar satellite and of William Toll and John Lee at Taylor University and Sean Lev-Tov of Stanford University for developing data analysis software. This work was supported by NASA under grant NAG5-11573 at Stanford University and grant NAG5-11982 at Taylor University.

[59] Arthur Richmond thanks Mei-Ching Fok and Finn Soraas for their assistance in evaluating this paper.

References

Anderson, B. J., R. B. Decker, and N. P. Paschalidis (1997), On the onset of nonadiabatic particle motion in the near-Earth magnetotail, *J. Geophys. Res.*, *102*, 17,553.

Blake, J. B., et al. (1995), Comprehensive energetic particle distribution experiment on POLAR, in *The Global Geospace Mission*, edited by C. T. Russell, Kluwer Acad., Norwell, Mass.

Carpenter, D. L., and R. R. Anderson (1992), An ISEE/Whistler model of equatorial electron density in the magnetosphere, *J. Geophys. Res.*, *97*, 1097.

Chen, M., M. Schulz, L. Lyons, and D. Gorney (1993), Stormtime transport of ring current and radiation belt ions, *J. Geophys. Res.*, *98*, 3835.

Cornwall, J. M., F. V. Coroniti, and R. M. Thorne (1970), Turbulent loss of ring current protons, *J. Geophys. Res.*, *75*, 4699.

Daglis, I. A., R. M. Thorne, W. Baumjohann, and S. Orsini (1999), The terrestrial ring current: Origin, formation, and decay, *Rev. Geophys.*, *37*, 407.

Daglis, I. A., J. U. Kozyra, Y. Kamide, D. Vassiliadis, A. S. Sharma, M. W. Liemohn, W. D. Gonzalez, B. T. Tsuratani, and G. Lu (2003), Intense space storms: Critical issues and open disputes, *J. Geophys. Res.*, *108*(A5), 1208, doi:101029/2002JA009722.

Erlandson, R. E., and A. J. Ukhorskiy (2001), Observations of electromagnetic ion cyclotron waves during geomagnetic storms: Wave occurrence and pitch angle scattering, *J. Geophys. Res.*, *106*, 3883.

Feldstein, Y. I., L. A. Dremukhina, U. Mall, and J. Woch (2000), On the two-phase decay of the Dst-variation, *Geophys. Res. Lett.*, *27*, 2813.

Fok, M.-C., J. U. Kozyra, A. F. Nagy, and T. E. Cravens (1991), Lifetime of ring current particles due to coulomb collisions in the plasmasphere, *J. Geophys. Res.*, *96*, 7861.

Fok, M.-C., T. E. Moore, J. U. Kozyra, G. C. Ho, and D. C. Hamilton (1995), Three-dimensional ring current decay model, *J. Geophys. Res.*, *100*, 9619.

Fok, M.-C., T. E. Moore, and M. E. Greenspan (1996), Ring current development during storm main phase, *J. Geophys. Res.*, *101*, 15,311.

Fu, S. Y., B. Wilken, Q. G. Zong, and Z. Y. Pu (2001), Ion composition variations in the inner magnetosphere: Individual and collective storm effects in 1991, *J. Geophys. Res.*, *106*, 29,683.

Hauge, R., and F. Soraas (1975), Precipitation of >115 keV protons in the evening and forenoon sectors in relation to magnetic activity, *Planet. Space Sci.*, *23*, 1141.

Jordanova, V. K., L. M. Kistler, J. U. Kozyra, G. U. Khazanov, and A. F. Nagy (1996), Collisional losses of ring current ions, *J. Geophys. Res.*, *101*, 111.

Jordanova, V. K., C. J. Farrugia, R. M. Thorne, G. B. Khazonov, G. D. Reeves, and M. F. Thomsen (2001), Modeling ring current proton precipitation by electromagnetic ion clclotron waves during the May 14–15, 1997, storm, *J. Geophys. Res.*, *106*, 7.

Kennel, C. F., and H. E. Petschek (1966), Limit on stably trapped particle fluxes, *J. Geophys. Res.*, *71*, 1.

Khazanov, G. V., K. V. Gamayunov, V. K. Jordanova, and E. N. Krivorutsky (2002), A self-consistent model of the interacting ring current ions and electromagnetic ion cyclotron waves, initial results: Waves and precipitating fluxes, *J. Geophys. Res.*, *107*(A6), 1085, doi:10.1029/2001JA00180.

Kistler, L. M., F. M. Ipavich, D. C. Hamilton, G. Gloeckler, B. Wilken, G. Kremser, and W. Studemann (1989), Energy spectra of the major ion species in the ring current during geomagnetic storms, *J. Geophys Res.*, *94*, 3579.

Kozyra, J. U., M.-C. Fok, E. R. Sanchez, D. S. Evans, D. C. Hamilton, and A. F. Nagy (1998), The role of precipitation losses in producing the rapid early recovery phase of the great magnetic storm of February 1986, *J. Geophys. Res.*, *103*, 6801.

Liemohn, M. W., J. U. Kozyra, V. K. Jordanova, G. V. Khazanov, M. F. Thomsen, and T. E. Cayton (1999), Analysis of early phase ring current recovery mechanisms during geomagnetic storms, *Geophys. Res. Lett.*, *26*, 2845.

Liemohn, M. W., J. U. Kozyra, C. R. Clauer, and A. J. Ridley (2001), Computational analysis of the near-Earth magnetospheric current system during two-phase decay storms, *J. Geophys. Res.*, *106*, 29,531.

Lundblad, J. A., and F. Soraas (1978), Proton observations supporting the ion cyclotron wave heating theory of SAR arc formation, *Planet. Space Sci.*, *26*, 245.

Sergeev, V. A., E. M. Sazhina, N. A. Tsyganenko, J. A. Lundblad, and F. Soraas (1983), Pitch angle scattering of energetic protons in the magnetotail current sheet as the dominant source of their isotropic precipitation into the nightside ionosphere, *Planet. Space Sci.*, *31*, 1147.

Smith, P. H., R. A. Hoffman, and T. A. Fritz (1976), Ring current proton decay by charge exchange, *J. Geophys. Res.*, *81*, 2701.

Soraas, F., K. Aarsnes, J. A. Lundblad, and D. S. Evans (1999), Enhanced pitch angle scattering of protons at mid-latitude during geomagnetic storms, *Phys. Chem. Earth, Part C*, *24*, 287.

Soraas, F., K. Aarsnes, K. Oksavil, and D. S. Evans (2002), Ring current intensity estimated from low-altitude proton observations, *J. Geophys. Res.*, *107*(A7), 1149, doi:10.1029/2001JA000123.

Walt, M., and H. D. Voss (2001), Losses of ring current ions by strong pitch angle scattering, *Geophys. Res. Lett.*, *28*, 3839.

Williams, D. J., and L. R. Lyons (1974), The proton ring current and its interaction with the plasmapause: Storm recovery phase, *J. Geophys. Res.*, *79*, 4195.

Yahnina, T. A., A. G. Yahnin, J. Kangas, and J. Manninen (2000), Proton precipitation related to Pc1 pulsations, *Geophys. Res. Lett.*, *27*, 3575.

H. D. Voss, Department of Physics, Taylor University, 236 West Reade Avenue, Upland, IN 46989-1001, USA. (hnvoss@tayloru.edu)

M. Walt, Starlab, Stanford University, Packard Building, Stanford, CA 94395, USA. (walt@nova.stanford.edu)